ISSN 1063-7834, Physics of the Solid State, 2017, Vol. 59, No. 12, pp. 2387–2393. © Pleiades Publishing, Ltd., 2017.
Original Russian Text © A.A. Shibkov, M.A. Zheltov, M.F. Gasanov, A.E. Zolotov, 2017, published in Fizika Tverdogo Tela, 2017, Vol. 59, No. 12, pp. 2363–2369.

## MECHANICAL PROPERTIES, PHYSICS OF STRENGTH, AND PLASTICITY

# Mechanism of Low-Frequency Discrete Acoustic Emission during Intermittent Creep of Aluminum Alloy

**A. A. Shibkov*, M. A. Zheltov, M. F. Gasanov, and A. E. Zolotov**

*Derzhavin Tambov State University, Internatsional'naya ul. 33, Tambov, 392000 Russia*

**e-mail: shibkov@tsu.tmb.ru*

Received May 10, 2017

**Abstract**—A correlation between the dynamics of deformation bands and the discrete acoustic emission during the intermittent creep of the AlMg6 alloy using a high-speed video recording with a time resolution to 50 μs has been studied. A trigger of a macroscopic deformation step in the creep curve is the nucleation and the broadening of the primary deformation band that generates a characteristic acoustic emission signal with duration of several milliseconds. The results confirm the mechanism of generating an acoustic emission signal related to the cooperative dislocations outcrop on the specimen external surface.

**DOI:** 10.1134/S1063783417120289

## 1. INTRODUCTION

Plastic deformation of solids occurs, as is known, intermediatedly and nonuniformly at various scales. At the macroscopic scale, the intermittent plastic deformation is manifested as repeated stress drops during deformation with a given rate $\dot{\varepsilon}_0$ = const in a rigid testing machine (the Portevin–Le Chatelier (PLC) effect) [1] or as deformation steps upon loading at constant rate $\dot{\sigma}_0$ = const in a soft testing machine (the Savart–Masson effect [2]), and/or as deformation "explosions" upon creep tests (the "ladder" effect [3]). The latter phenomenon usually called the intermittent creep is manifested as sharp steps with amplitude from 0.1 to 6% and more at the first and the second stages of creep in polycrystalline Ni–Cr alloys [4–6], austenitic steels [7–9], and aluminum alloys [10–12].

Deformation steps and stress drops in the tensile stress–strain curves are accompanied by localization of plastic deformation in macrolocalized deformation bands [12, 13]. According to the accepted point of view, these plastic instabilities are due to a dynamic strain ageing, i.e., dynamic interaction of mobile dislocations with diffused impurity atoms [14]. The intermittent plastic flow and the formation of deformation bands influence many properties of materials: they decrease the metal plasticity, the coefficient of rate sensitivity, and the fracture stress. The plasticity loss caused by strain localization can cause premature fracture of a loaded structural material. Because of this, a monitoring of deformation bands is an important problem from the scientific and practical points of view. An appropriated review of experimental methods of studying the dynamics of deformation bands in the conditions of the PLC effect was presented in [15]; there it was underlined that the acoustic emission (AE) method has an advantage as compared to other methods for the measure the amount of events provided by an intermittent plastic flow. In addition, the continuous acoustic monitoring of dislocation avalanches gives information on their dynamics for time ranges ~1 μs–1 ms in the conditions of the PLC effect [16–24].

It was noted in [25] that the plastic deformation localization must increase low-frequency components in an AE spectrum, because of an increase in the correlation between dislocation jumps during their thermoactivated motion in a solid solution, for example, because of avalanche-like depinning of dislocations from impurity atmospheres. Thus, the AE spectrum shift toward lower-frequency range is an indicator of deformation localization at higher scales, which was experimentally confirmed in [19, 26, 27]. This work presents the experimental results of the in situ study of the correlation between the dynamics of deformation bands and the low-frequency (in the frequency range 10–1000 Hz) acoustic response during the intermittent creep of an aluminum–magnesium alloy.

## 2. EXPERIMENTAL

We studied a commercial aluminum–magnesium AlMg6 alloy (6.15 wt % Mg, 0.65 wt % Mn, 0.25 wt % Si, 0.21 wt % Fe). Plane specimens in the shape of two-side blades with the gage part sizes of 6 × 3 × 0.5 mm were cut from a cold-rolled strip along the rolling direction. Before the test, the specimens were annealed at 450°C for 1 h with subsequent quenching

in air. As a result, this heat treatment gave the microstructure with an average grain size of ~10 μm. The detailed studies of the initial structure of the alloy were presented in [28].

To study the intermittent creep, we used a set of in situ methods [29] on the base of a soft deformation test machine that was specially designed for studying the instable deformation of metals. The soft machine is a lever device loaded by pouring water with a given flow rate in a vessel fastened on the level end. This machine is capable to perform tension tests of metallic specimens at a constant rate of increasing the load and also in the creep conditions. The creep tests were carried out at room temperature. The specimens were aged at 20°C for two days before the test to stabilize their structures.

The force response was measured using a Zernik A3-C3-100kg-3V force sensor with a sensitivity of 1.5 μV/*N*. The specimen deformation was measured using a Riftec optical laser triangulation displacement transducer accurate to 1.5 μm in the frequency range 0–2 kHz. The measured loads and deformations were recorded at a rate of 2 kHz. The video recording of the surface was performed using a FASTCAM Mini UX50/100 (Photron) high-speed digital video camera in synchronism with the measurements of the deformation and the force; the video camera was used to optically monitor the processes of formation and propagation of deformation bands at a speed to 20000 frames/s. The processing of the video recording data was the subtraction of subsequent video film frames using a special computer program [30].

The acoustic response for the intermittent creep of the AlMg6 alloy specimen was studied using a miniature (6mm in diameter) acoustic detector made on the base of barium titanate; the detector was mounted, via an oil layer, on the immobile blade of the specimen connected to the base (testing machine mount). The channel of recording the AE signal consisted of a broadband high-resistance preamplifier ($R_{in} = 10^{12}$ Ω, $C_{in} = 20$ pF, pass band $1–10^6$ Hz), a commutator, a multichannel analog-to-digital converter (ADC), and a computer. The signals of AE, the displacement transducers, the force sensors, and the signal of the high-speed video camera in the form of a meander at the recording frequency were synchronically recorded using four ADC channels at a clock frequency of 100 kHz on a channel.

## 3. RESULTS AND DISCUSSION

Figure 1 depicts a typical example of the synchronic recording of the data of measurements of the deformation, the stress, and the acoustic emission signal during spontaneous nucleation and development of a deformation step with amplitude of ~4% in the creep curve at stress $\sigma_0 = 217$ MPa that is significantly higher than the conventional yield strength $\sigma_{0.2} \approx$ 160 MPa in the AlMg6 alloy. The shape of the deformation step, i.e., the time dependence of strain increment $\Delta\varepsilon(t)$ at the step front is close to the sigmoid logistic curve with the characteristic rise time (the front duration) ~600 ms (Fig. 1, curve *1*). The force response (Fig. 2, curve *2*) contains more than one dozen of stress jumps with amplitudes ~3–10 MPa and a pulse rise time of ~1–3 ms. This intermittent force response similar to the PLC effect is related to the inertia of the "machine–specimen" system [12, 31, 32].

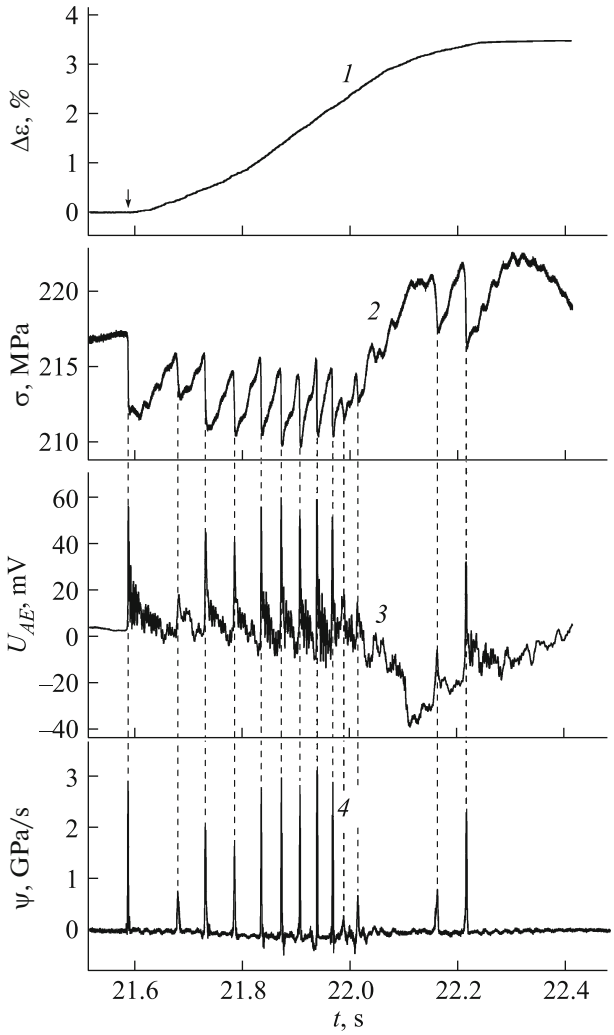


**Fig. 1.** (*1*) Macroscopic step Δε in the creep curve at stress $\sigma_0 = 217$ MPa, (*2*) force response σ, (*3*) acoustic emission signal $U_{AE}$, and (*4*) function ψ is the time dependence of the absolute value of the time derivative of the force response. The arrow shows the moment of nucleation of the primary deformation band.

As was found in [12], each of the stress drops is related, as a rule, to the appearance of one deformation band that has a form of an expanding neck. The evolution of each of the bands is characterized by two subsequent stages; fast and slow. The fast stage with

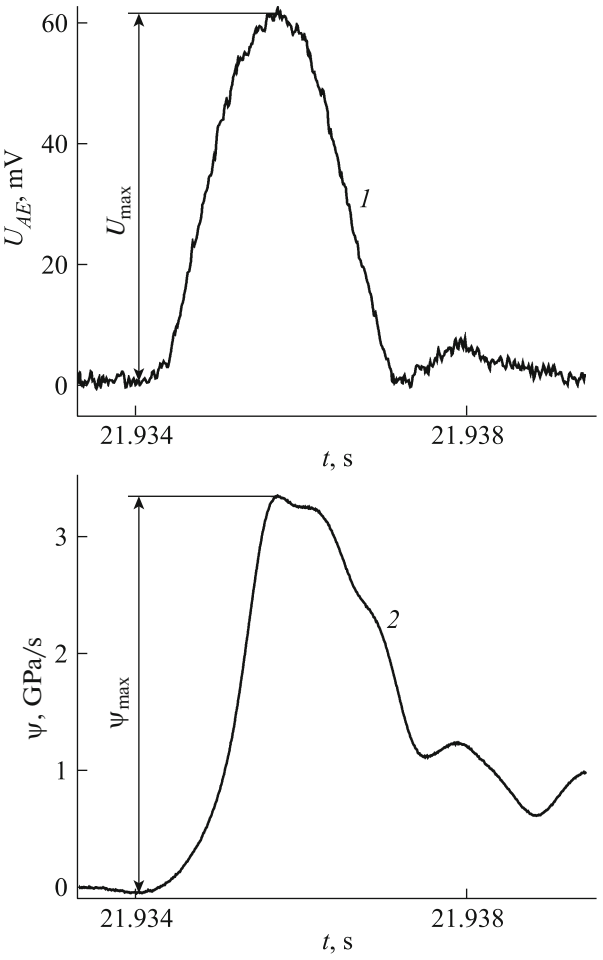


**Fig. 2.** (*1*) Typical example of the first oscillation with amplitude $U_{max}$ of the AE burst caused by the formation of a deformation band and (*2*) corresponding peak of function ψ with amplitude $\psi_{max}$.

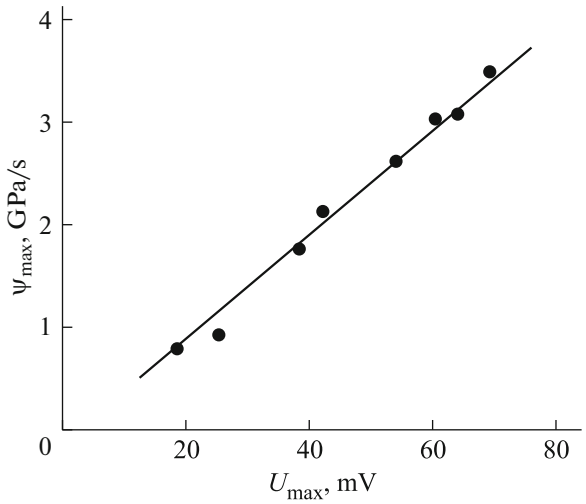


**Fig. 3.** Dependence $\psi_{max}(U_{max})$. Correlation coefficient with a linear approximation $k = 0.9985$.

duration ~1–3 ms is accompanied by a sharp discharge of the mechanical system with amplitude to ~10 MPa, whereas the slow stage of broadening with duration of ~10–100 ms is accompanied by continuous recovering of the stress almost to the initial value.

As is seen from Fig. 1, each of the stress drops is accompanied by the AE signal burst that is a sequence of damping with a damping time ~30 ms. The first acoustic oscillation in the AE burst structure occurs simultaneously with a sharp discharge of the mechanical system and, therefore, to the initial fast stage of the evolution of the deformation band with duration ~1–3 ms. The subsequent damping oscillations in the AE burst structure occurs simultaneously with continuous stress recovering that is related to the slow stage (without any irregularities) of broadening of the deformation band [12]. Because of this, the damping oscillations after the first oscillation with the maximum amplitude in the AE burst structure (Fig. 1, curve *3*) are not related to any relaxation processes in the deformed material; they are likely to be related to the excitation of eigenmodes of the "machine–specimen" mechanical system. Actually, the fundamental frequency of damping oscillations in the AE signal (~300 Hz), according to the data of ballistic tests, coincides with the eigenmode of the test machine at the tensile stress of ~200 MPa. Thus, it can be concluded that only the first acoustic oscillation in the AE burst structure contains information on the dynamics of deformation band, namely, on the nucleation and the initial fast stage of the band evolution.

Let us consider another temporal series that reflects the macroscopic plastic instability, namely, the absolute value of the derivative with respect to the force response time $\psi(t) = |d\sigma(t)/dt|$, along with the AE signal. This temporal series was used to characterize the plastic flow jumps in Al–Mg alloys in the conditions of the PLC effect [33–37]. In Fig. 1, curves *3* and *4* demonstrate the correlation between the AE signal $U_{AE}(t)$ and function $\psi(t)$. As is seen from Fig. 2, the form of the first oscillation in the AE signal (curve *1*) is similar to the form of the $\psi(t)$ function pulse (curve *2*) observed during the initial fast stage of the evolution of the deformation band. Figure 3 demonstrates the near-linear dependence of the amplitude $\psi_{max}$ of the peak of function $\psi(t)$ on amplitude $U_{max}$ of the first oscillation in the AE signal with a comparatively high correlation coefficient ($k = 0.9985$). This implies that the AE signal caused by the nucleation and fast stage of the evolution of the deformation band gives information on the rate of varying the force response. Therefore, the significance of the measurement of the acoustic emission under conditions of the intermittent creep is that the AE method gives information in real time on the discharge jumps, peaks of function $\psi(t)$, and the amount of diffraction bands

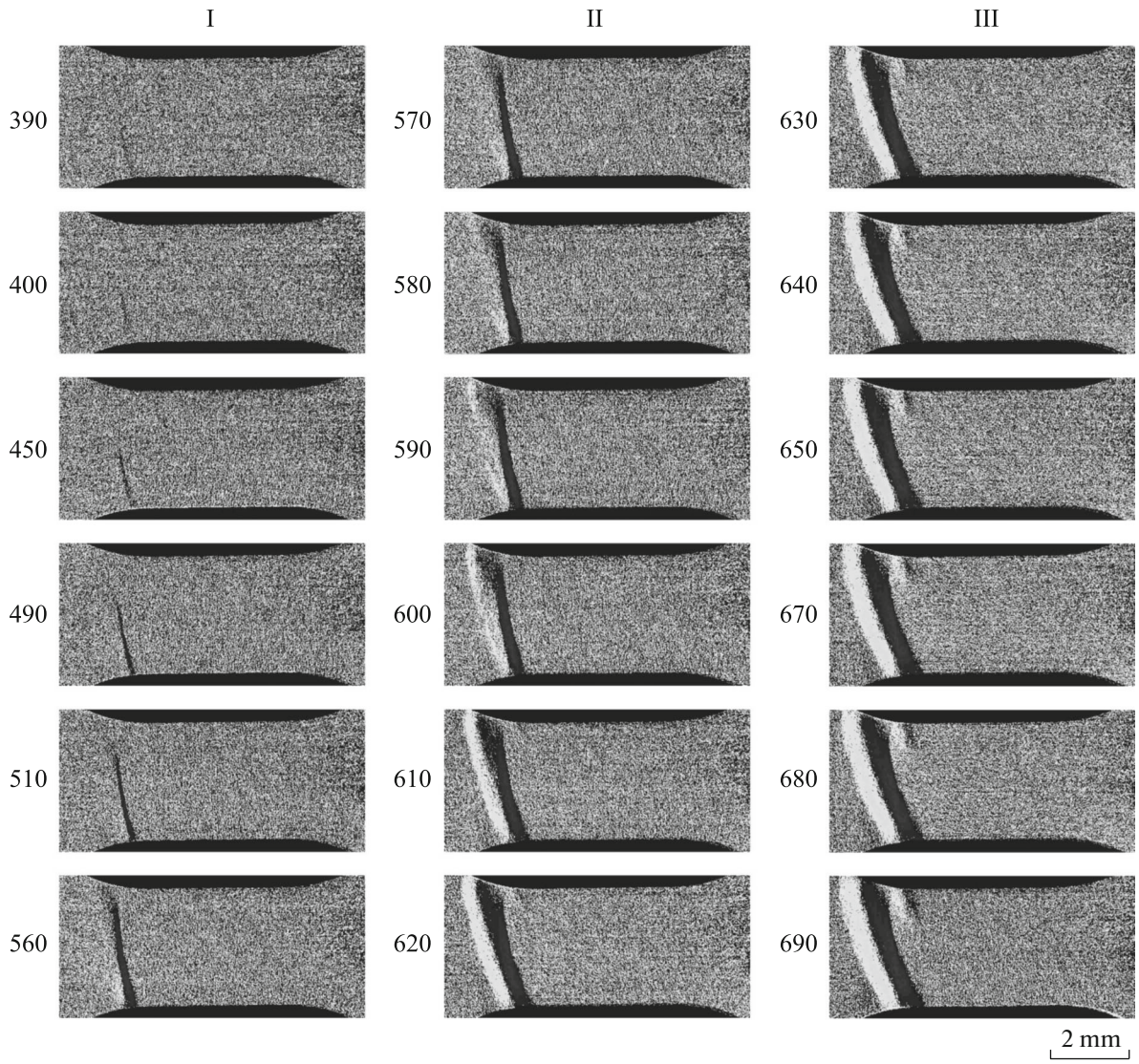


**Fig. 4.** Results of computer processing the data of video recording of the growth of the primary deformation band. Roman numerals note the main stages of the evolution of the band: I is the stage of the transverse growth of the band "nucleus," i.e., the incomplete band of the localized displacement, II is the stage of the sharp widening the band, and III is the stage of slow widening the band. The numbers indicate the numbers of frames. The speed of the video recording is 20 000 frames/s (the time interval between frames is 50 μs).

without a force sensor and video camera, for example, under conditions of the operating a structural material.

According to the data of [12], the main mechanism of developing the macroscopic deformation step in the creep curve, when each new deformation band, except for the primary band, nucleates at the boundary of preceding band. The primary band nucleates spontaneously in a random position at the gage length of the specimen and is a trigger of developing the deformation step.

Consider the initial stage of the evolution of the primary band in more detail to study the peculiarities of the correlation between the nucleation of the plastic deformation localization and the characteristics of the AE signal. Figure 4 shows the data of the video recording of the initial stage of the evolution of the primary band at a speed of recording of 20 000 frames/s synchronized with the AE signal. As is seen from Fig. 4, the plastic deformation is localized, first, as a nucleus of a deformation band that forms at one of the specimen edge (frame 1). Then, this band nucleus in the form of a narrow wedge of the deformed material grows into the specimen bulk at some angle to the tension axis for 3–10 ms, which agrees qualitatively with the grow of the nucleus of the B-type PLC band in Al–Cu and Al–Mg deformed in the rigid test machine [38–41].

At the moment of time when a band nucleus intersects all the cross-section and outcrop to the opposite specimen surface, the formation of the deformation

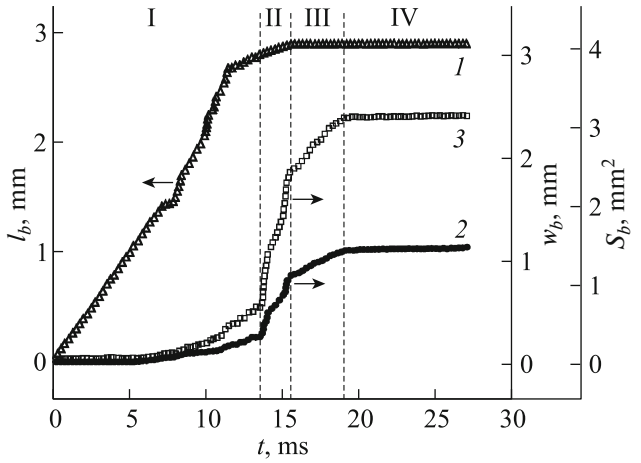


**Fig. 5.** Time dependences of (*1*) $l_b$, (*2*) width $w_b$, and (*3*) area $S_b$ of the primary deformation band (trigger of the development of the macroscopic step in the creep curve of the AlMg6 alloy. The minimum time interval between the experimental points is 50 μs.

band is ended and its broadening starts. Figure 5 shows the kinetic curves characterizing the growth of the primary deformation band, time dependences of length (*1*) $l_b$, (*2*) width $w_b$, and (*3*) area $S_b$ of the band. As the analysis of the correlations of these curves with the force and acoustic responses, the highest correlation coefficient is observed for the time dependence of the band area $S_b(t)$ with corresponding responses. We can separate, at least, four main time stages of the kinetics and morphology of the band with respect to rate of increasing the band area (Fig. 4): stage I of the transverse growth of the band nucleus with a top rate $v_t$ to ~1 m/s (frames 390–570) that is ended by the outcrop of the band to the specimen surface opposite from the source (frame 570); at this stage, the completed (intersecting all cross-section) localized displacement band; stage II of the avalanche-like broadening band at a rate $v_w$ to 30 cm/s (frames 570–610) when the rate of the band area growth is maximum (~1 mm$^2$/ms); at this completing stage, the localized displacement band is transformed to an expanding neck (Fig. 2 in [42]); stage III of slow continuous broadening of the deformation band, and stage IV of a quasi-stationary state of the band. A finer structure of the band kinetics related to nonuniform growth of the band at stage I and the formation of a small secondary band-satellite at the right boundary of the broadened primary band at stage III (frames 620–680).

Stage I of the growth of the band-nucleus (Fig. 6) is accompanied by a gradual increase in the AE signal. The sharp increase in the AE signal takes place only at stage II after the outcrop of the localized displacement band to the opposite specimen surface and subsequent avalanche-like increase in the band area. At this stage of developing the band, the absolute values of all

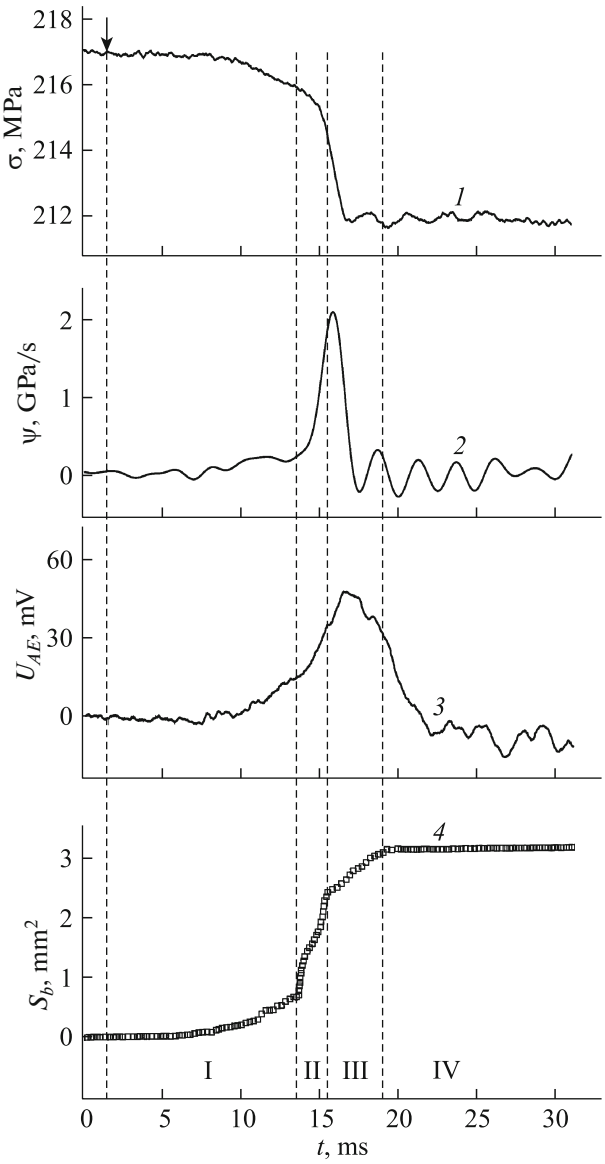


**Fig. 6.** Time dependences of (*1*) stress σ, (*2*) function ψ, (*3*) acoustic emission signal $U_{AE}$, and (*4*) the primary band area $S_b$. The arrow indicates the moment of nucleating the primary band, according to the data of the high-speed video recording. Roman numerals I–IV note the stages of the evolution of the band.

responses become maximal. The correlation coefficient between functions $S_b(t)$ and acoustic signal $U_{AE}(t)$ at the two first stages is $k_{US} = 0.9857$, that is slightly higher than the correlation coefficient with the force response $k_{U\sigma} = 0.9673$. Thus, the sharp increase in the AE signal takes place only after the formation of the through band (completed band) as a result of motion of large amount of dislocations over all the cross-section and their outcrops to the external specimen surface.

The common idea of AE accompanying the intermittent PLC flow relates the AE signal bursts with the nucleation of deformation bands [17, 18, 20, 22]; at the same time, the results of this work show that the nucleation and the evolution of a deformation band generate a comparative weak AE signal, and the main contribution to the acoustic burst is due to the formation of the through band that is accompanied by the outcrop of dislocations to the external specimen surface. This observation confirms the mechanism of generating an AE signal as a result of the dislocation outcrops to the specimen surface [43].

Thus, our studies of the correlation between the dynamics of the deformation bands and AE signals during the intermittent creep of the AlMg6 alloy show that the first oscillation with duration ~3–10 ms in the burst structure of the AE signal is related to the formation of the primary deformation band that is a trigger of the development of the macroscopic deformation step with a pulse rise time of ~0.5 s in conditions of the intermittent creep. Thus, this first acoustic oscillation can be considered as an acoustic precursor of the macroscopic deformation step that can be used for triggering force devices of suppressing deformation instability, for example, for starting a current generator for suppressing a deformation jump and the development of deformation bands by electric current [44].

## 4. CONCLUSIONS

The correlation between the intermittent creep and the discrete low-frequency (in the frequency range 10–1000 Hz) acoustic emission in commercial AlMg6 alloy with a time resolution to 50 μs has been studied for the first time. The nucleation and fast broadening of the primary deformation band are triggers of the development of the deformation step in the creep curve that generate a characteristic AE signal with duration of ~3–10 ms. It is assumed that the most probable mechanism of generation of an acoustic signal–precursor is the formation of the primary through deformation band due to the nucleation and motion of a large amount of dislocations over all cross-section and their outcrop on the external surface of the specimen. The observed correlations between the AE signals and the processes of formation of deformation bands can be a scientific basis for developing the methods of early diagnostics of plastic deformation localization in alloys demonstrating the intermittent creep.

## ACKNOWLEDGMENTS

This work was supported by the Russian Science Foundation, project no. 15-12-00035.

## REFERENCES

1. A. Portevin and F. Le Chatelier, C.R. Acad. Sci. Paris **176**, 507 (1923).
2. F. Savart, Ann. Chim. Fhys. **65**, 337 (1837).
3. E. N. Andrade, Proc. R. Soc. **84**, 1 (1910).
4. R. L. Klueh and J. F. King, Scr. Metall. **13**, 205 (1979).
5. R. L. Klueh and J. F. King, J. Nucl. Mater. **98**, 173 (1981).
6. R. L. Klueh, Mater. Sci. Eng. **54**, 65 (1982).
7. T. L. Silveira and S. N. Monteiro, Metall. Trans. A **10**, 1795 (1979).
8. S. N. Monteiro, T. L. Silveira, and I. LeMay, Scr. Metall. **15**, 957 (1971).
9. V. K. Sikka and S. V. David, Metall. Trans. A **12**, 883 (1981).
10. J. Kariya, H. Oikawa, and S. Karashina, Trans. Jpn. Inst. Met. **14**, 327 (1973).
11. M. Hamersky, P. Lukac, Z. Trojanova, and E. Pink, Mater. Sci. Eng. A **148**, 7 (1991).
12. A. A. Shibkov, M. F. Gasanov, M. A. Zheltov, A. E. Zolotov, and V. I. Ivolgin, Int. J. Plast. **86**, 37 (2016).
13. K. Chihab, Y. Estrin, L. P. Kubin, and J. Vergnol, J. Scr. Metall. **21**, 203 (1987).
14. L. P. Kubin, C. Fressengeas, and G. Ananthakrishna, in *Dislocations in Solid*s, Ed. by F. R. N. Nabarro and M. S. Duesbery (Elsevier, Amsterdam, 2002), p. 101.
15. A. J. Yilmaz, Sci. Technol. Adv. Mater. **12**, 1 (2011).
16. F. Chmelik, A. Ziegenbein, H. Neuhauser, and P. Lukac, Mater. Sci. Eng. A **324**, 200 (2002).
17. F. Chmelik, F. B. Klose, H. Dierke, J. Sachl, H. Neuhauser, and P. Lukac, Mater. Sci. Eng. A **462**, 53 (2007).
18. M. M. Krishtal and D. L. Merson, Phys. Met. Metallogr. **81**, 104 (1996).
19. M. M. Kpishtal, A. K. Khpustalev, A. A. Pazuvaev, and I. S. Demin, Deform. Razrush. Mater. **1**, 28 (2008).
20. M. A. Lebyodkin, T. A. Lebedkina, F. Chmelik, T. T. Lamark, Y. Estrin, C. Fressengeas, and J. Weiss, Phys. Rev. B **79**, 174114 (2009).
21. M. A. Lebyodkin, N. P. Kobelev, Y. Bougherira, D. Entemeyer, C. Fressengeas, V. S. Gornakov, T. A. Lebedkina, and I. V. Shashkov, Acta Mater. **60**, 3729 (2012).
22. I. V. Shashkov, M. A. Lebyodkin, and T. A. Lebedkina, Acta Mater. **60**, 6842 (2012).
23. M. A. Lebyodkin, I. V. Shashkov, and T. A. Lebedkina, Phys. Rev. E **88**, 042402 (2013).
24. J. Kumar, R. Sarmah, and G. Ananthakrishna, Phys. Rev. B **92**, 144109 (2015).
25. A. Vinogradov and A. Lasarev, Scr. Mater. **66**, 745 (2012).
26. A. V. Vinogradov, V. Patlan, and S. Hashimoto, Philos. Mag. **81**, 1427 (2001).
27. A. Lazarev and A. Vinogradov, J. Acoust. Emission **27**, 144 (2009).
28. A. A. Shibkov, A. A. Mazilkin, S. G. Ppotasova, D. V. Mikhlik, A. E. Zolotov, M. A. Zheltov, and A. V. Shuklinov, Deform. Razrush. Mater. **5**, 24 (2008).

29. A. A. Shibkov, M. A. Lebedkin, M. A. Zheltov, V. V. Skvortsov, M. A. Zheltov, and A. V. Shuklinov, Zavod. Lab. **71**, 20 (2005).
30. A. A. Shibkov, A. E. Zolotov, and M. A. Zheltov, Bull. Russ. Acad. Sci.: Phys. **76**, 85 (2012).
31. A. A. Shibkov, A. E. Zolotov, M. A. Zheltov, A. A. Denisov, and M. F. Gasanov, Tech. Phys. **59**, 508 (2014).
32. A. A. Shibkov, A. E. Zolotov, M. A. Zheltov, M. F. Gasanov, and A. A. Denisov, Phys. Solid State **56**, 881 (2014).
33. M. S. Bharathi, G. Ananthakrishna, C. Fressengeas, L. P. Kubin, and M. Lebyodkin, Phys. Rev. Lett. **87**, 165508 (2001).
34. M. S. Bharathi, M. Lebedkin, G. Ananthakrishna, C. Fressengeas, and L. P. Kubin, Acta Mater. **50**, 2813 (2002).
35. M. A. Lebyodkin and Y. Estrin, Acta Mater. **53**, 3403 (2005).
36. M. A. Lebyodkin and T. A. Lebedkina, Phys. Rev. E **73**, 036114 (2006).
37. M. A. Lebyodkin and T. A. Lebedkina, Phys. Rev. E **77**, 026111 (2008).
38. W. Tong, H. Tao, N. Zhang, and L. G. Hector, Scr. Mater. **53**, 87 (2005).
39. G. F. Xiang, Q. C. Zhang, H. W. Liu, X. P. Wu, and X. Y. Ju, Scr. Mater. **56**, 721 (2007).
40. V. V. Gorbatenko, V. I. Danilov, and L. B. Zuev, Tech. Phys. **62**, 395 (2017).
41. A. A. Shibkov and A. E. Zolotov, *Actual Problems of Mechanics of Deformable Solids. Nonlinear Dynamics on Unstable Plastic Metal Deformatio*n (Tambov. Gos. Univ. im. G. R. Derzhavina, Tambov, 2010) [in Russian].
42. A. A. Shibkov and A. E. Zolotov, JETP Lett. **90**, 370 (2009).
43. V. D. Natsik, JETP Lett. **8**, 198 (1968).
44. A. A. Shibkov, A. A. Denisov, M. A. Zheltov, A. E. Zolotov, and M. F. Gasanov, Mater. Sci. Eng. A **610**, 338 (2014).

*Translated by Yu. Ryzhkov*